Split-miniSOG for spatially detecting intracellular protein-protein interactions by correlated light and electron microscopy

Daniela Boassa*[,1], Sakina P. Lemieux[2], Varda Lev-Ram[2], Junru Hu[1], Qing Xiong[2], Sebastien Phan[1], Mason Mackey[1], Ranjan Ramachandra[1], Ryan E. Peace[4], Stephen R. Adams[2], Mark H. Ellisman[1,3,#] and John T. Ngo*[,4,5#]

[1] Department of Neurosciences, National Center for Microscopy and Imaging Research, University of California, San Diego, La Jolla CA 92093
[2] Department of Pharmacology, University of California, San Diego, La Jolla CA 92093
[3] Department of Bioengineering, University of California, San Diego, La Jolla CA 92093
[4] Department of Biomedical Engineering and Biological Design Center, Boston University, Boston, MA 02215
[5]Lead contact

* To whom correspondence should be addressed: dboassa@ucsd.edu; jtngo@bu.edu
[#] Co-senior Authors

SUPPLEMENTAL FIGURES AND LEGENDS

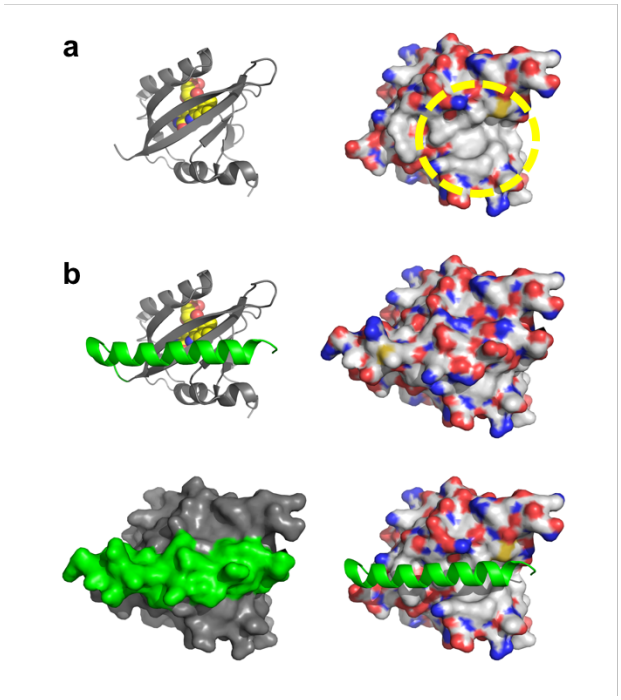
a
b

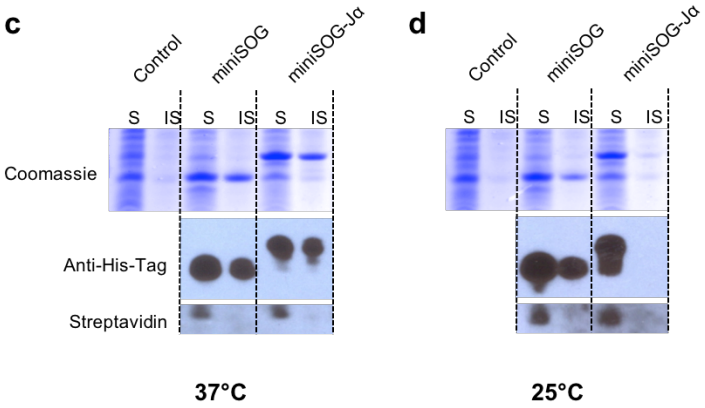
c
Control
miniSOG
miniSOG-Jα
S
IS
S
IS
S
IS
Coomassie
Anti-His-Tag
Streptavidin
37°C
d
Control
miniSOG
miniSOG-Jα
S
IS
S
IS
S
IS
25°C

Supplementary Figure 1 (Related to Figure 1) | Inclusion of the Jα-helix increases the solubility of miniSOG when rapidly and highly overexpressed in *E. coli*. (**a**) Structures of the LOV2 domain from oat (PDB: 2V0U) shown without Jα-helix residues. A small, solvent-exposed hydrophobic patch is highlighted (yellow dotted line, right image). Cartoon images are displayed with FMN shown as spheres (left image). Coloring by atom (right image): C is light gray, O is red, N is blue, and S is yellow. (**b**) Structures of the same domain displayed with the Jα-helix shown (green), which sequesters the surface-exposed hydrophobic patch. (**c-d**) Comparison of inclusion body formation between miniSOG and miniSOG-Jα. Briefly, His-tagged versions of the proteins were over-expressed in *E. coli* from an IPTG-inducible promoter at either 37° or 25°C. Expression at both temperatures led to high levels of recombinant protein (~20% of total cellular protein content). Soluble and insoluble cell fractions were subsequently prepared and analyzed by Coomassie staining of SDS-PAGE gels as well as by Western blotting with an anti-His-tag antibody. In cells that were induced at 25°C, miniSOG-Jα was completely soluble and was not detected in the insoluble fraction. To assess the quality of the cell fractionation procedure, Western membranes were stripped and re-probed with streptavidin-HRP in order to reveal biotin-carboxyl carrier protein (~17 kDa), a soluble and endogenously biotinylated *E. coli* protein. Streptavidin-HRP signal was detected only in soluble fractions, indicating a successful separation of soluble and insoluble proteins.

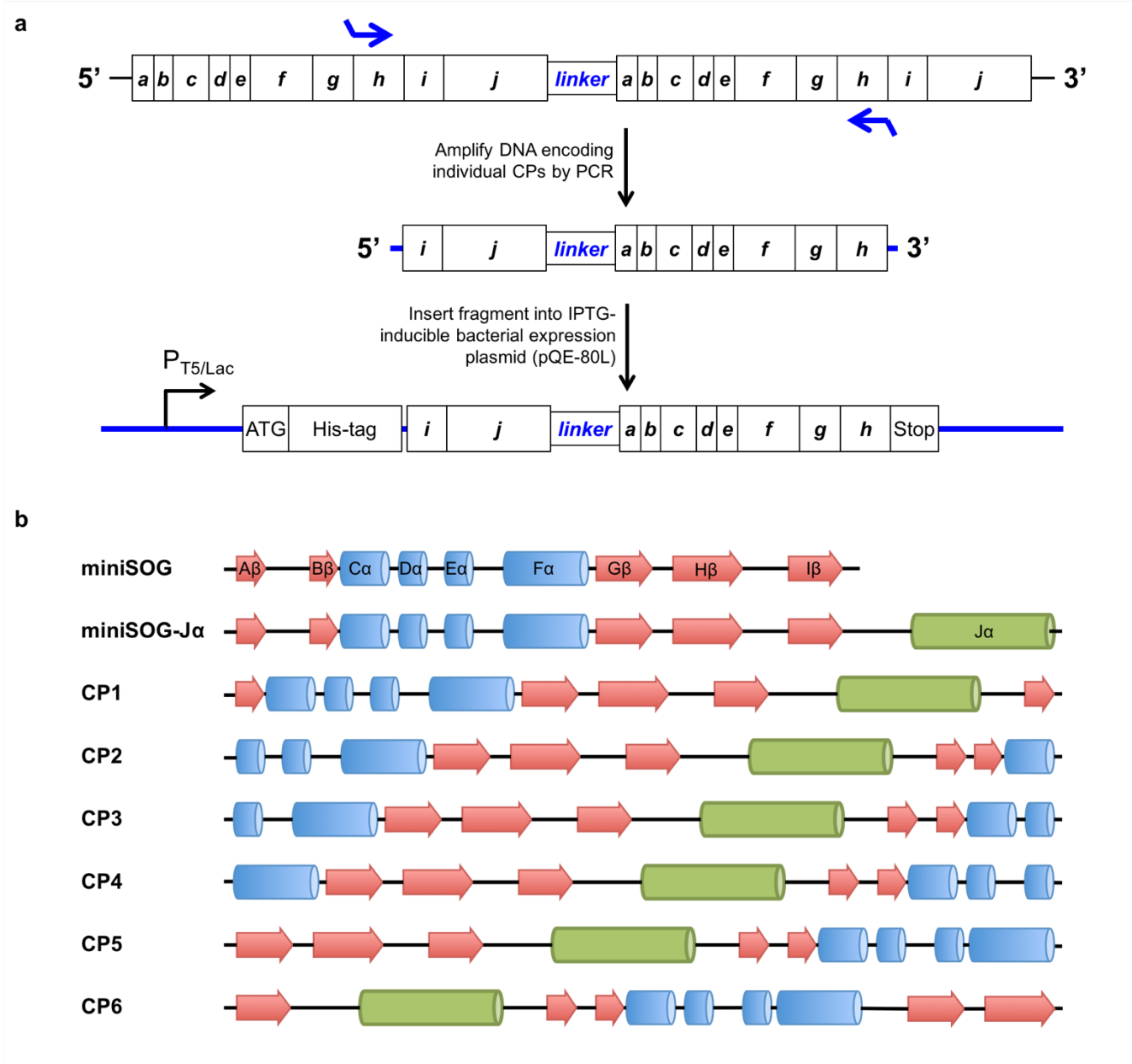
a
5'
a b c d e f g h i j
linker
a b c d e f g h i j
3'
Amplify DNA encoding individual CPs by PCR
5'
i j
linker
a b c d e f g h
3'
Insert fragment into IPTG-inducible bacterial expression plasmid (pQE-80L)
P T5/Lac
ATG
His-tag
i j
linker
a b c d e f g h
Stop
b
miniSOG
Aβ Bβ Cα Dα Eα Fα Gβ Hβ Iβ
miniSOG-Jα
Jα
CP1
CP2
CP3
CP4
CP5
CP6

Supplementary Figure 2 (Related to Figure 1) | Generation of miniSOG-Jα CP pool. (**a**) Schematic of the cloning strategy used to generate DNA sequences encoding the individual CPs. A non-repetitive DNA sequence encoding a miniSOG-Jα tandem dimer was used as a template from which monomeric CP genes were amplified using PCR. Generation of the CP6 gene is depicted. (**b**) Secondary structural elements of miniSOG, miniSOG-Jα, and CP1 – CP6. Beta sheets are shown as arrows, and helices are shown as cylinders. The Jα-helix is shown as a green cylinder.

a

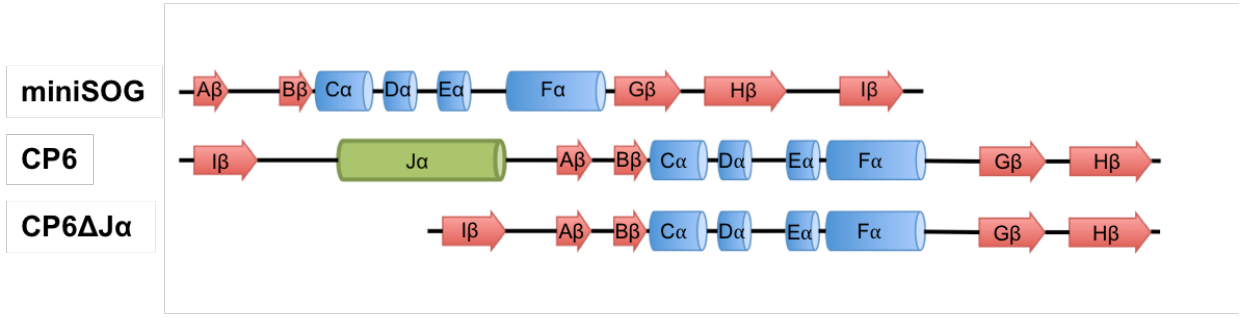
miniSOG
CP6
CP6ΔJα
Aβ
Bβ
Cα
Dα
Eα
Fα
Gβ
Hβ
Iβ
Jα

b

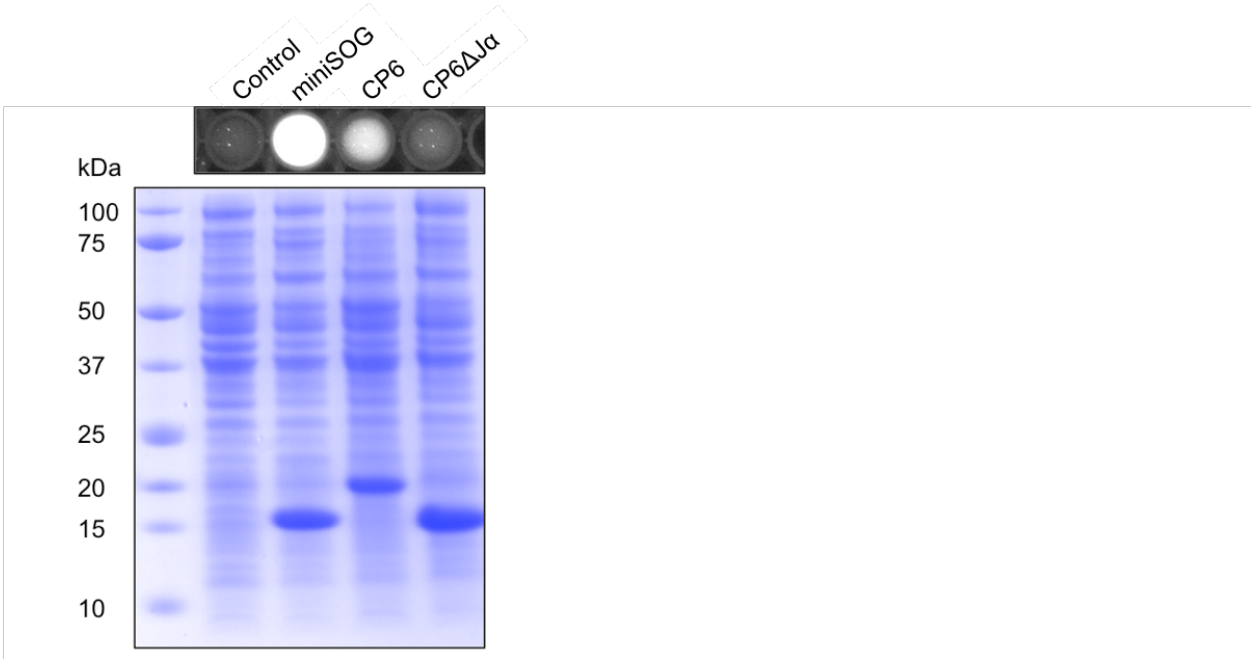
Control
miniSOG
CP6
CP6ΔJα
kDa
100
75
50
37
25
20
15
10

Supplementary Figure 3 (Related to Figure 1) | The Jα-helix aids in the proper folding of CP6. (**a**) Schematic representation of the secondary structural elements of miniSOG, CP6, and CP6ΔJα. (**b**) Fluorescence detection of *E. coli* cells expressing the indicated proteins (top) and Coomassie-stained SDS-PAGE gel of corresponding total protein extracts, including both the soluble and insoluble forms of each species (bottom). Calculated protein masses of the His-tagged proteins: miniSOG = 15.23 kDa, CP6 = 19.11 kDa, CP6ΔJα = 15.34 kDa.

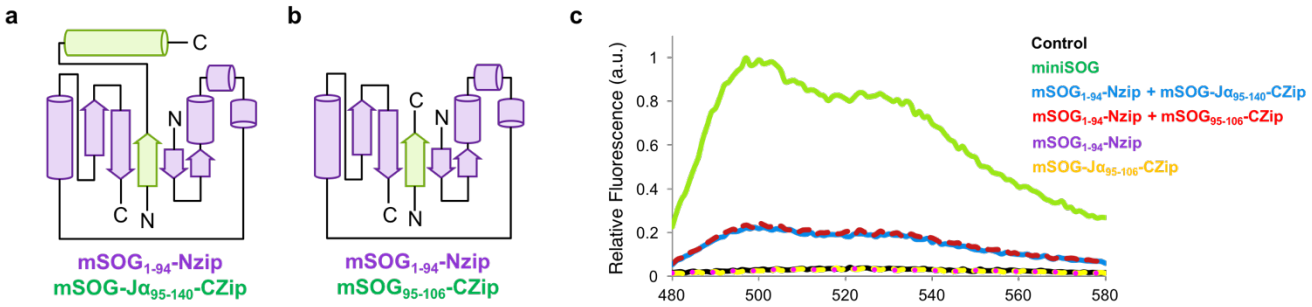
a
C
N
C
N
mSOG1-94-Nzip
mSOG-Jα95-140-CZip
b
C
N
C
N
mSOG1-94-Nzip
mSOG95-106-CZip
c
Relative Fluorescence (a.u.)
1
0.8
0.6
0.4
0.2
0
480
500
520
540
560
580
Control
miniSOG
mSOG1-94-Nzip + mSOG-Jα95-140-CZip
mSOG1-94-Nzip + mSOG95-106-CZip
mSOG1-94-Nzip
mSOG-Jα95-106-CZip

Supplementary Figure 4 (Related to Figure 1) | Comparison of $mSOG_{1-94}$/mSOG-$J\alpha_{95-140}$ and $mSOG_{1-94}$ and mSOG-$_{95-106}$ in *E. coli.* (**a**) Topology of $mSOG_{1-94}$ (purple) and mSOG-$J\alpha_{95-140}$ (green) tagged with leucine zipper sequences (Nzip and Czip). (**b**) Topology of $mSOG_{1-94}$ (purple) and $mSOG_{95-106}$ (green) tagged with Nzip and Czip. (**c**) Expression of individual miniSOG fragments in *E. coli* is insufficient for upregulation of cellular FMN biosynthesis. Fluorescence emission spectra from *E. coli* cells expressing leucine zipper sequences (Nzip and Czip) tagged with miniSOG/miniSOG-Jα fragments. Independent expression of $mSOG_{1-94}$-Nzip, mSOG-$J\alpha_{95-140}$-Czip did not result in detectable fluorescence above background. Co-expression of $mSOG_{1-94}$-Nzip and mSOG-$J\alpha_{95-140}$-Czip (blue line), or $mSOG_{1-94}$-Nzip and $mSOG_{95-106}$-Czip (red line) resulted in comparable levels of fluorescence with spectral profiles resembling that of miniSOG.

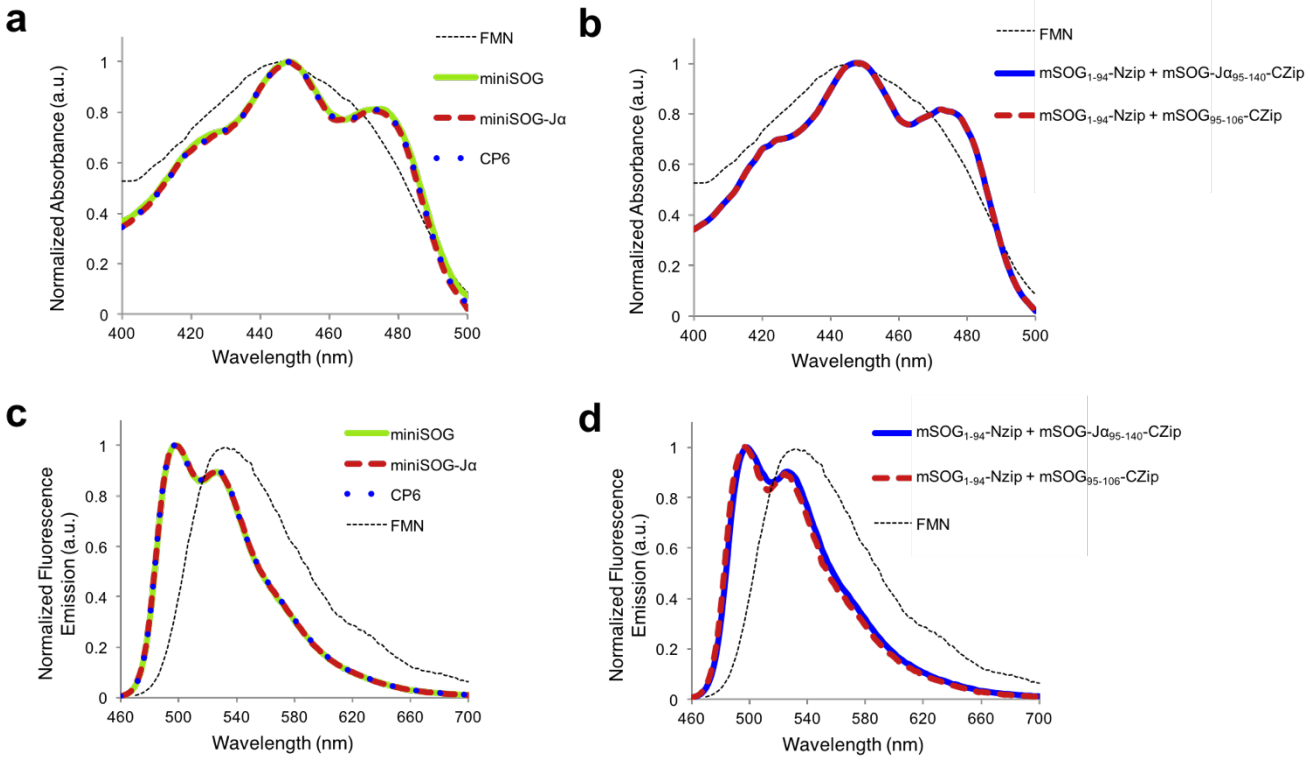
a
Normalized Absorbance (a.u.)
Wavelength (nm)
FMN
miniSOG
miniSOG-Jα
CP6
b
Normalized Absorbance (a.u.)
Wavelength (nm)
FMN
mSOG1-94-Nzip + mSOG-Jα95-140-CZip
mSOG1-94-Nzip + mSOG95-106-CZip
c
Normalized Fluorescence Emission (a.u.)
Wavelength (nm)
miniSOG
miniSOG-Jα
CP6
FMN
d
Normalized Fluorescence Emission (a.u.)
Wavelength (nm)
mSOG1-94-Nzip + mSOG-Jα95-140-CZip
mSOG1-94-Nzip + mSOG95-106-CZip
FMN

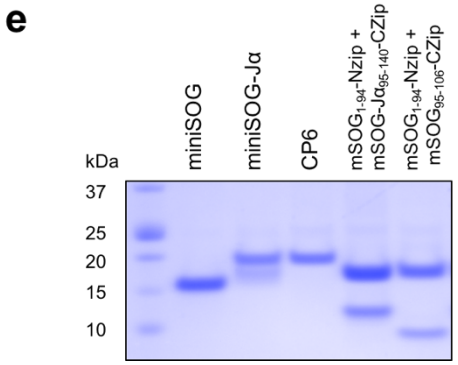
e
kDa
37
25
20
15
10
miniSOG
miniSOG-Jα
CP6
mSOG1-94-Nzip + mSOG-Jα95-140-CZip
mSOG1-94-Nzip + mSOG95-106-CZip

Supplementary Figure 5 (Related to Figure 1) | FMN remains bound to miniSOG-Jα, CP6, and reconstituted complexes following purification. Normalized absorption and fluorescence emission spectra of free FMN and purified miniSOG, miniSOG-Jα, CP6 (**a, c**), as well as $mSOG_{1-94}$-Nzip/mSOG-$Jα_{95-140}$-Czip and $mSOG_{1-94}$-Nzip/mSOG-$_{95-106}$-Czip complexes (**b, d**). LOV-domain bound FMN exhibits characteristic vibronic structure (multiple peaks) that is not observed with the free chromophore. (**e**) Coomassie-stained SDS-PAGE gel of the purified proteins used to collect the spectra shown in (a-d). Calculated protein masses: miniSOG (with myc and His-tag) = 15.23 kDa, miniSOG-Jα (with His-tag) = 19.11 kDa, CP6 (with His-tag) = 19.11 kDa, $mSOG_{1-94}$-Nzip (with His-tag) = 15.98 kDa, mSOG-$Jα_{95-140}$-Czip (untagged) = 10.66 kDa, mSOG-$_{95-106}$-Czip (untagged) = 6.90 kDa.

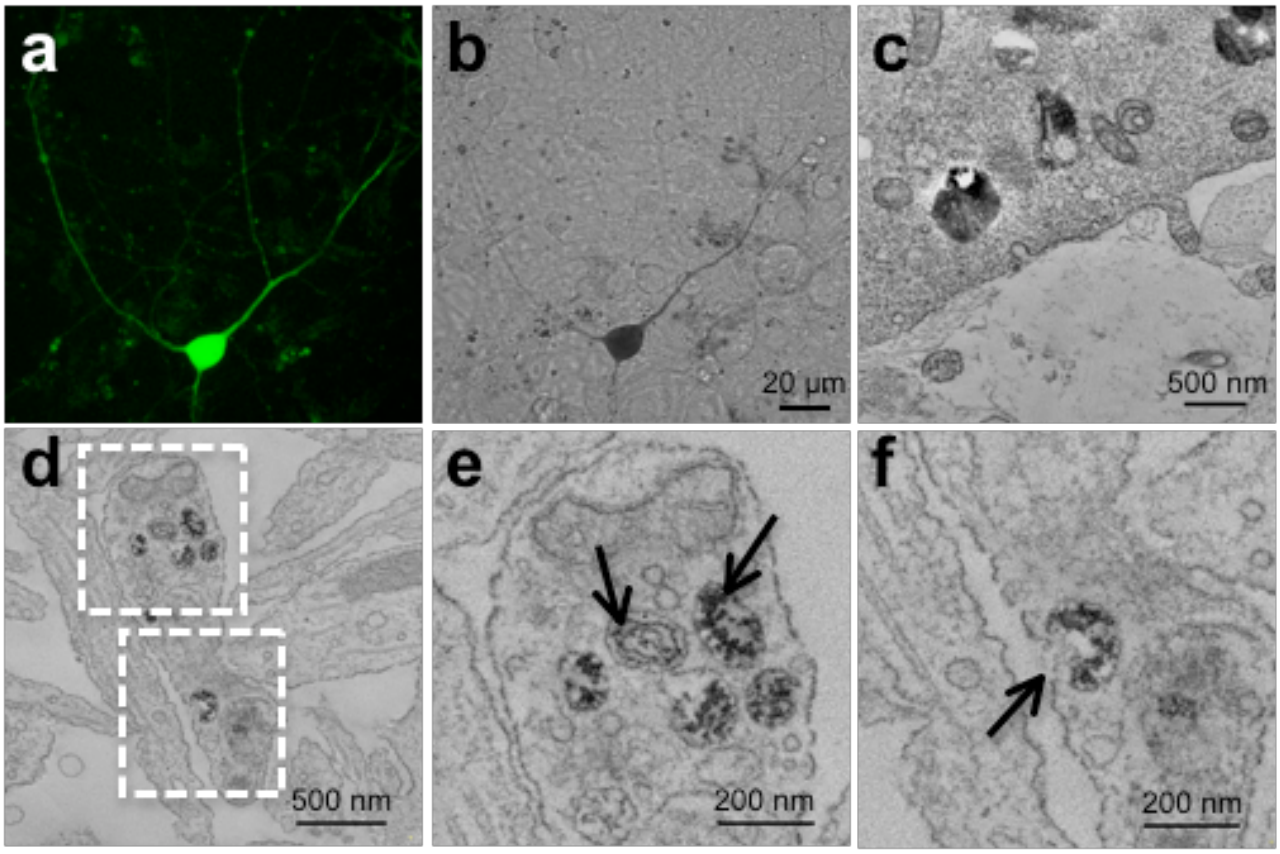
a
b
20 µm
c
500 nm
d
500 nm
e
200 nm
f
200 nm

Supplementary Figure 6 (Related to Figures 6 and 7) | Alpha-synuclein aggregates in the cell body and dendrites of neurons expressing the reconstituted miniSOG-Jα. (**a**) Confocal fluorescence image (maximum intensity projection) of live cultured neurons co-expressing the tagged α-syn proteins. A diffuse miniSOG fluorescent signal is observed throughout the neuron. Corresponding transmitted light image (**b**) was acquired post-fixation after 3 minutes and 30 seconds illumination in the presence of DAB. (**c-f**) TEM images of α-syn aggregates in the neuronal cell body (**c**) and dendrite (**d**). EM micrographs in (**e**) and (**f**) corresponds to white boxes in (**d**). Black arrow points at α-syn aggregates contained in membrane-limited organelles, fusing to the plasma membrane suggesting release to the extracellular compartment.

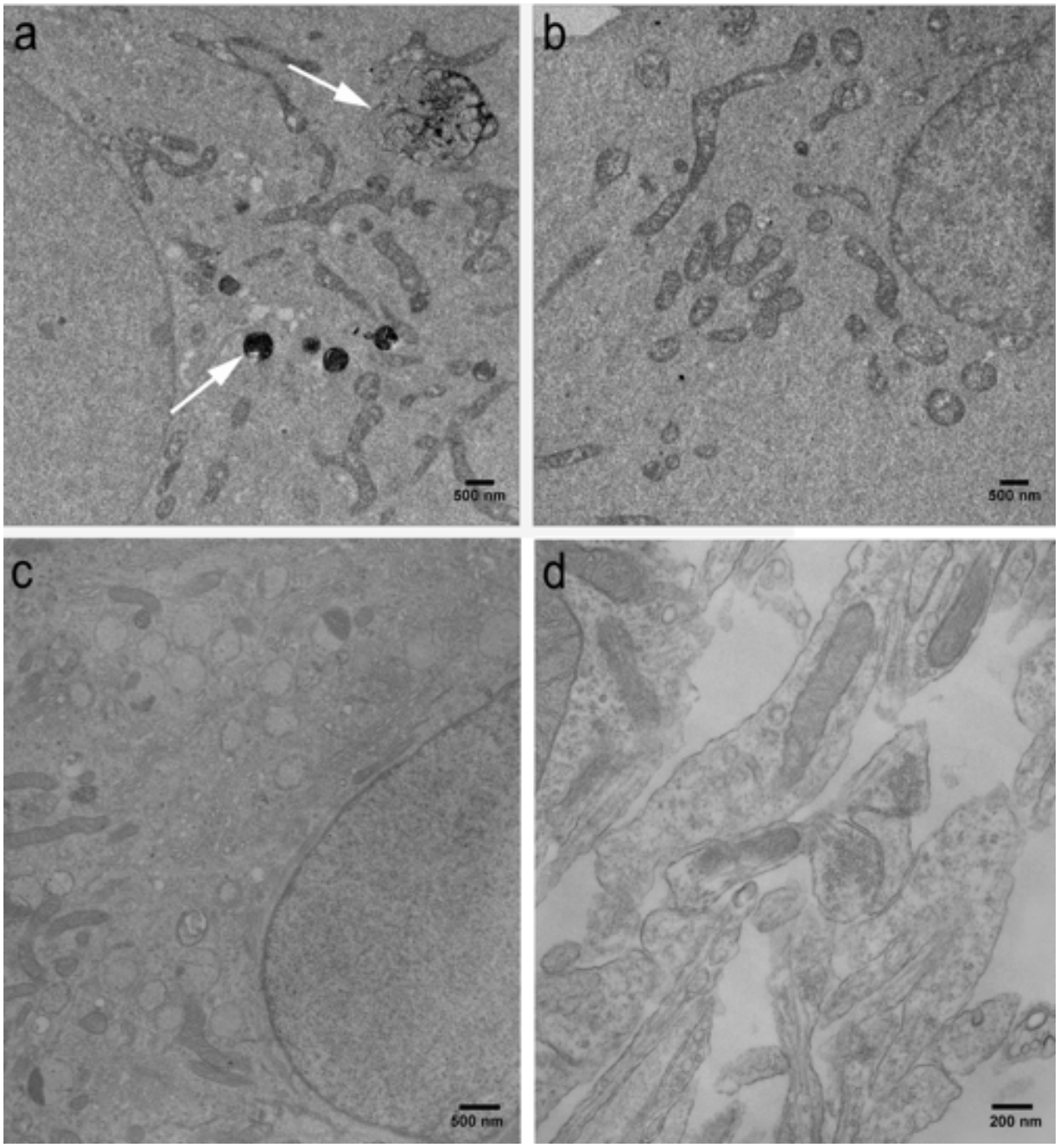
a
500 nm
b
500 nm
c
500 nm
d
200 nm

Supplementary Figure 7 (Related to Figures 6 and 7) | Comparison of photooxidized and non-photooxidized neurons expressing tagged α-syn proteins, and photooxidized untransfected neurons. EM micrographs of cell bodies of photooxidized neurons co-expressing $mSOG_{1-94}$ and $mSOG\text{-}J\alpha_{95-140}$ fusions of α-syn (**a**), non-photooxidized neurons co-expressing the same proteins (**b**), and photooxidized untransfected neurons (**c** and **d**). Stained α-syn aggregates (white arrows) are observed only in the photooxidized expressing neurons.

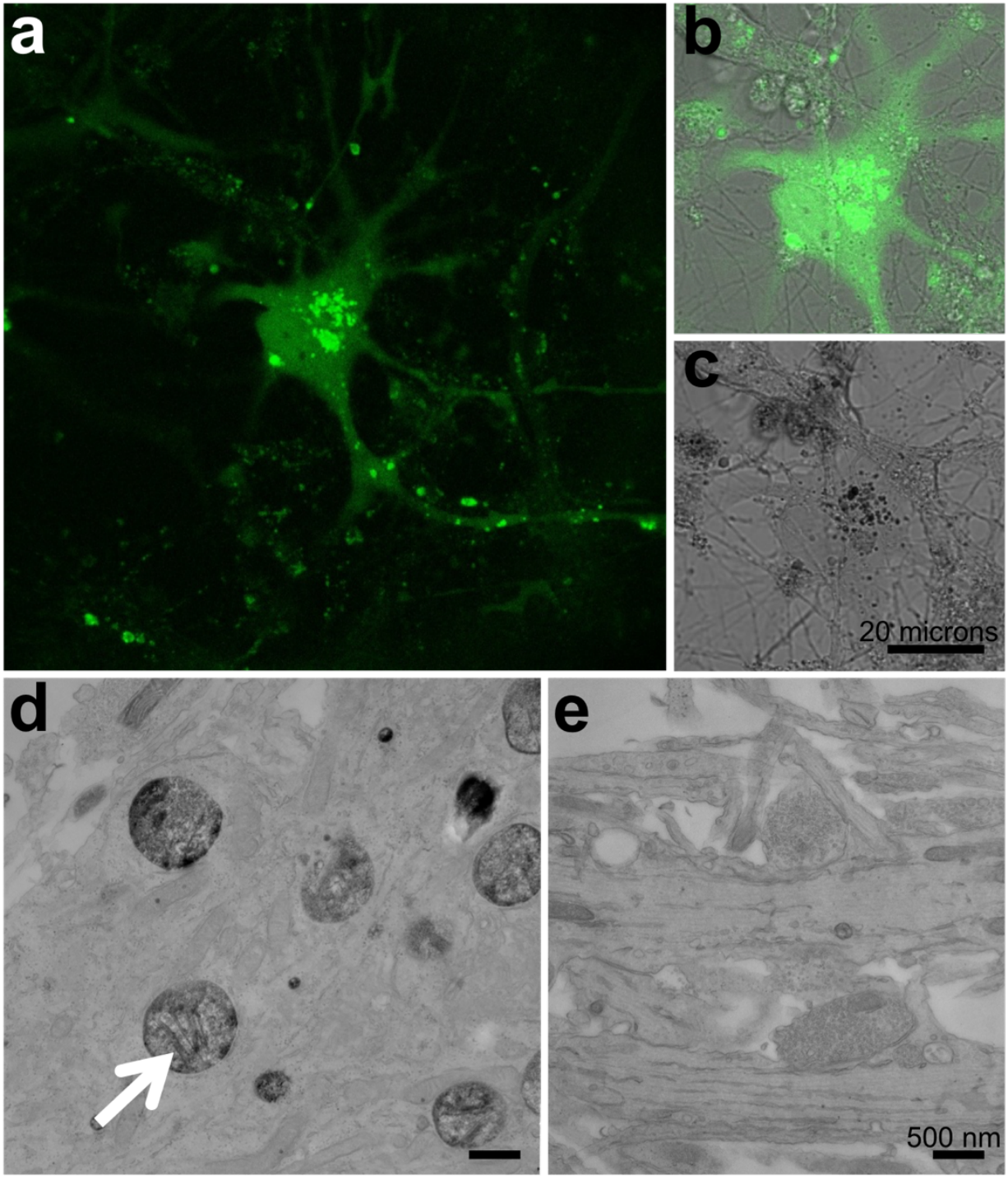
a
b
c
20 microns
d
e
500 nm

Supplementary Figure 8 (Related to Figures 6 and 7) | Oligomeric A53T familial mutant displays distribution characteristics similar to wild type α-syn. (**a**) Confocal fluorescence image of live cultured neurons co-expressing the A53T tagged proteins. (**b**) Fluorescence image overlaid on the transmitted light image before photooxidation of DAB. (**c**) Following photooxidation, the appearance of the optically visible DAB reaction product correlates with the detected reconstituted miniSOG fluorescence in (**a, b**). (**d**) Electron micrograph showing labeled α-syn fibrillar structures (white arrow) similar to the ones observed for wild type α-syn. (**e**) No labeling was observed at presynaptic terminals where α-syn aggregates were not detected.

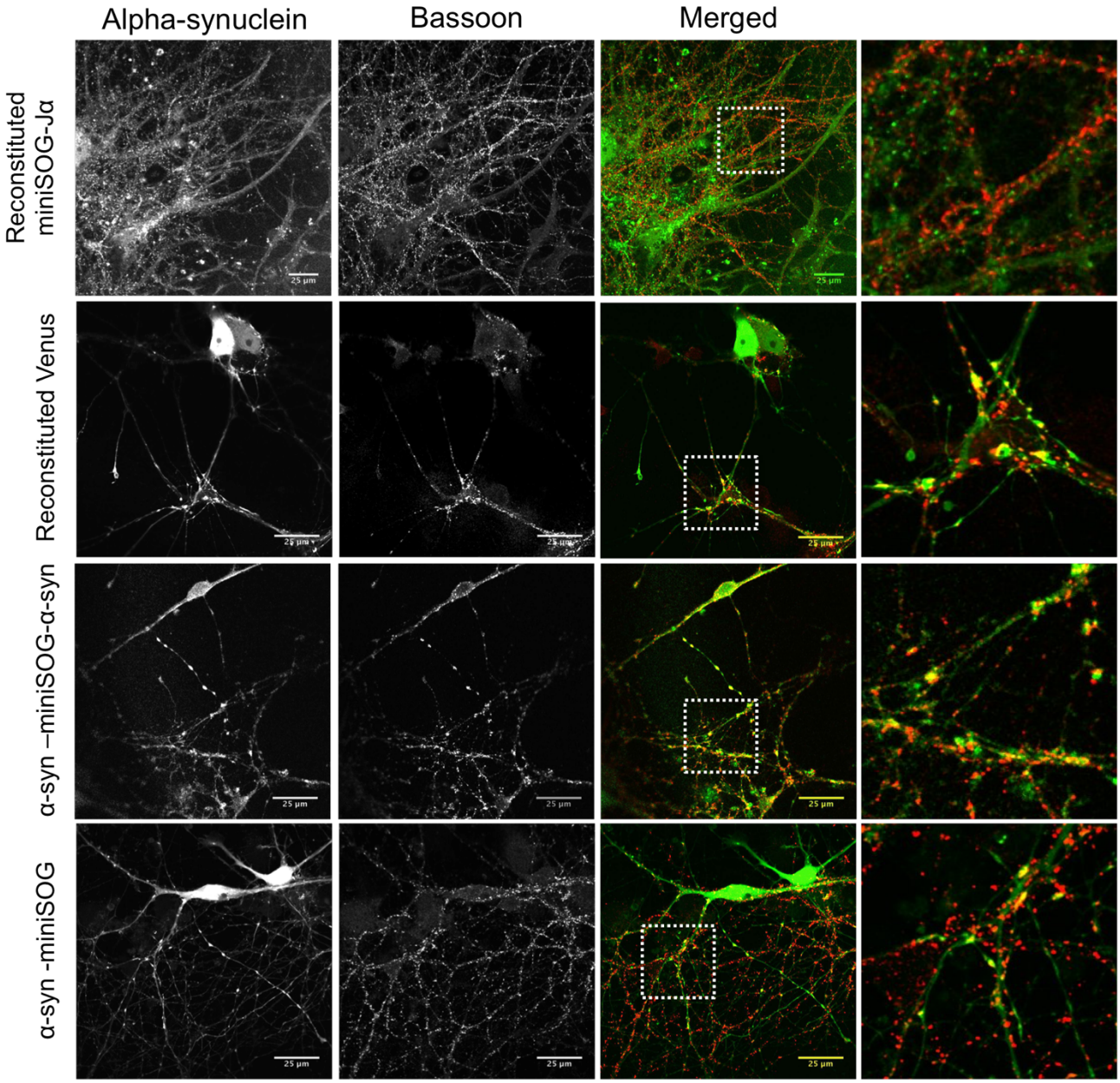
Alpha-synuclein
Bassoon
Merged
Reconstituted miniSOG-Jα
Reconstituted Venus
α-syn –miniSOG-α-syn
α-syn -miniSOG
25 µm

Supplementary Figure 9 (Related to Figures 6 and 7) | Oligomeric wild-type α-syn is excluded from presynaptic terminals. Confocal images (single confocal planes) showing the localization of the α-syn proteins fused to different tags (first column, intrinsic fluorescence), the labeling for Bassoon (presynaptic marker, second column), the merged images (third column) and an enlargement of the boxed areas shown in the white squares (last column to the right). Comparison of the reconstituted miniSOG-Jα fluorescence with reconstituted Venus reveals no localization of the reconstituted miniSOG-Jα to presynaptic terminals opposite to the reconstituted Venus. Fusion of two α-syn proteins to the N- and C- termini of miniSOG respectively (α-syn-miniSOG-α-syn) mimics the irreversible bonding of the reconstituted Venus and shows strong localization to presynaptic terminals. Single α-syn-miniSOG fusion proteins are observed at presynaptic terminals.

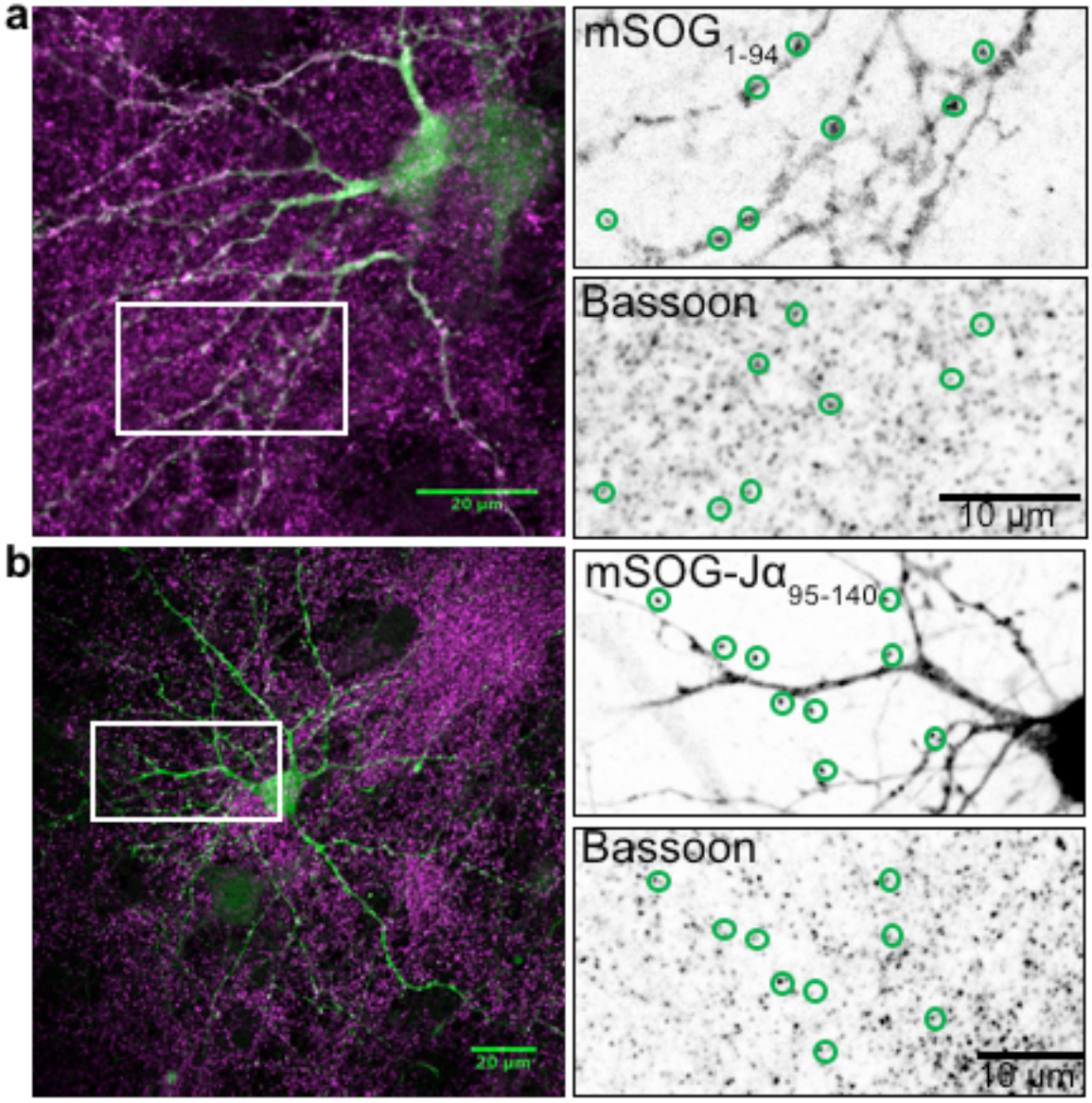
a
mSOG1-94
Bassoon
20 µm
10 µm
b
mSOG-Jα95-140
Bassoon
20 µm
10 µm

Supplementary Figure 10 (Related to Figures 6 and 7) | Individual α-syn proteins fused to each split-miniSOG-Jα-tagged fragment are localized to presynaptic terminals. (**a**) Confocal images of rat cortical neurons co-expressing α-syn fused to $mSOG_{1-94}$ (purple) and mSOG-$J\alpha_{95-140}$. Immunolabeling of $mSOG_{1-94}$ using an antibody that recognizes this fragment (RRX secondary antibody detection, shown in green in the merged image) and Bassoon (presynaptic marker, AX647 secondary antibody detection, shown in magenta in the merged image) demonstrate that the single-fragment fusions did not disrupt the ability of the α-syn proteins to traffic all the way to the presynaptic terminals. In the single channel confocal images (right column), the color table has been inverted for better visualization of the individual fluorescence channels. Green circles highlight corresponding labeling of α-syn proteins fused to each fragment colocalizing at presynaptic terminals. (**b**) Similarly, immunolabeling of mSOG-$J\alpha_{95-140}$ was done using an antibody to an additional epitope, HA, introduced in the fusion protein (RRX secondary antibody detection, shown in green in the merged image).

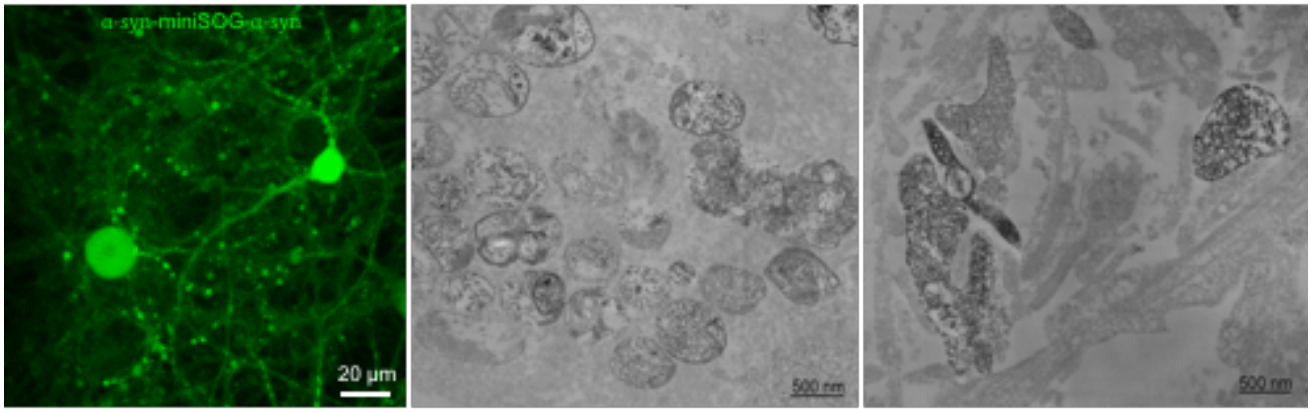
α-syn-miniSOG-α-syn
20 µm
500 nm
500 nm

Supplementary Figure 11 (Related to Figures 6 and 7) | Fusion of two α-syn proteins to the N- and C- termini of miniSOG respectively (α-syn-miniSOG-α-syn) mimics the irreversible bonding of the reconstituted Venus and shows strong labeling in presynaptic terminals. Confocal fluorescence image (left image) of live cultured neurons expressing the α-syn-miniSOG-α-syn proteins. Following 4 minutes photooxidation, electron micrographs show labeled α-syn aggregates in cell bodies (middle image) as well as strong labeling in presynaptic terminals (right image).

a

```
miniSOG   MEKSFVITDPRLPDNPIIFASDGFLELTEYSREEILGRNGRFLQGPETDQATVQKIRDAI 60
iLOV      IEKNFVITDPRLPDNPIIFASDGFLELTEYSREEILGRNARFLQGPETDQATVQKIRDAI 60
          :**.**********************************.********************

mSOG      RDQREITVQLINYTKSGKKFWNLLHLQPMRDQKGELQYFIGVQLDG 106
iLOV      RDQRETTVQLINYTKSGKKFWNLLHLQPVRDQKGELQYFIGVQLDG 106
          ***** **********************:*****************
```

b

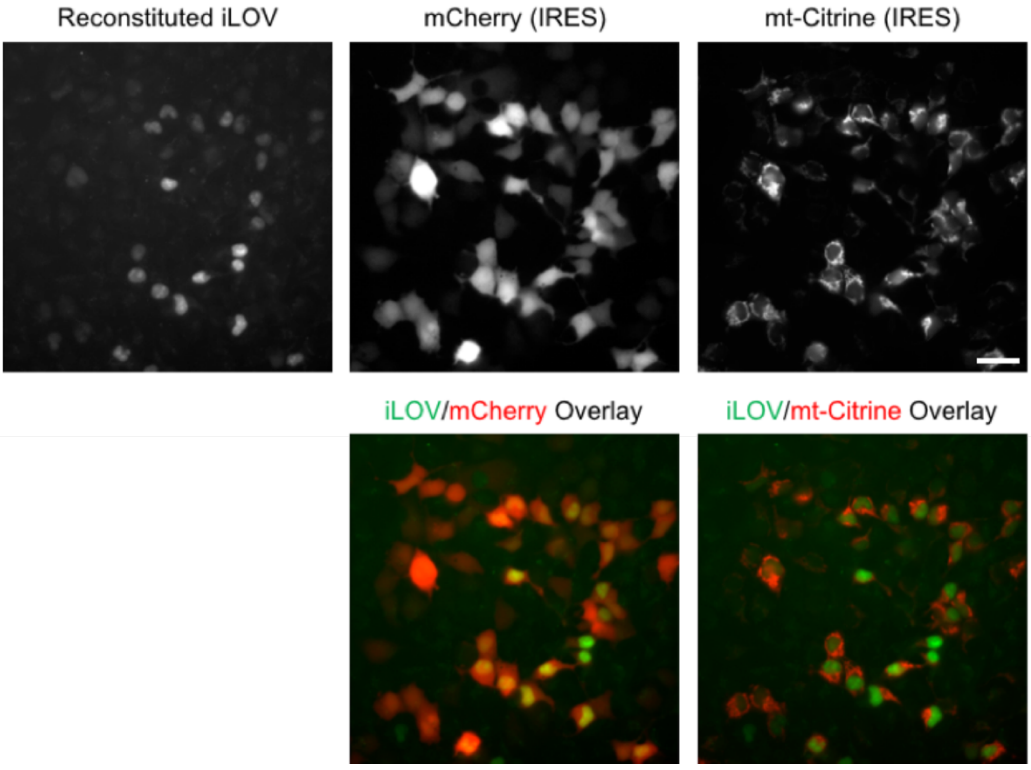

Supplementary Figure 12 (Related to Figure 1 and 2) | The identified split-site is transferable to the related LOV domain and fluorescent reporter protein iLOV. (**a**) Sequence alignment of miniSOG and iLOV. The red arrow indicates the split position identified in this work. (**b**) Fluorescence images of HEK293 co-expressing bFos and bJun domains tagged with split iLOV fragments. Signal from reconstituted iLOV complexes were confined to nuclei, and fluorescence from IRES-mCherry and IRES-mtCitrine confirmed uptake of the two constructs. Scale bar, 30 microns.

Protein/Protein Complex	Fluorescence Quantum Yield (Φ_F)
miniSOG	0.37*
miniSOG-Jα	0.34
CP6	0.36
$mSOG_{1-94}$-Nzip/mSOG-$Jα_{95-140}$-Czip	0.33
$mSOG_{1-94}$-Nzip/$mSOG_{95-106}$-Czip	0.29

Supplementary Table 1 (Related to Figure 1) | Fluorescence quantum yields of the proteins and reconstituted complexes described in this study. Values were calculated using purified miniSOG as the standard (*Shu, X., et al. *PLoS Biol.* **9**, e1001041 (2011)).

Supplementary Movie 1 (Related to Figures 6 and 7). 3D reconstruction of labeled protein inclusions containing fibrillar α-syn assemblies. Neurons co-expressing tagged α-syn chimeras were used for DAB photooxidation and subsequently processed for EM. A section of resin-embedded cells was cut to 250 nm and subsequently analyzed by electron tomography.